Eur. J. Hortic. Sci. | ISSN 1611-4426 print, 1611-4434 online | https://doi.org/10.17660/eJHS.2022/042 | © ISHS 2022

Original article

A growth model based on standardized growing degree days for hydroponic fresh cut tulip in solar greenhouses

Chen Cheng[1,2], Liping Feng[2], J.F. Bienvenido Barcena[3], Weidong Yu[4], Gen Li[5], Zhenfa Li[5] and Caihua Ye[6]

[1] Institute of Ecology, Lishui University, Lishui, Zhejiang, China
[2] College of Resources and Environment Sciences, China Agricultural University, Beijing, China
[3] Computer Science Department, University of Almeria, Almeria, Spain
[4] CMA/Henan Key Laboratory of Agro-meteorological Support and Applied Technique, Zhengzhou, China
[5] Tianjin Climate Center, Tianjin, China
[6] Beijing Municipal Climate Center, Beijing, China

Summary

Crop model is designed to dynamically and accurately simulate the growth process of crops, and according to people's demand for tulip, it is urgent to establish a simpler and more accurate growth model. In this study, tulip observation data was collected from experiments with six popular cultivars of tulip ('Pink Impression', 'Huge Pink', 'Lalibela', 'Daydream', 'Esmee' and 'Queen of Night'), which respectively represent different florescence of Early blossoming (EB), Middle blossoming (MB), Late blossoming (LB) and Very late blossoming (VB). Multi-sowing period treatment experiments were carried out in two growing seasons. The growth model for main organs morphology of tulip in this study is constructed by a new method named standardized growing degree days ($Stan_{GDD}$). The results showed that 1) Flowering stage is not affected by variety, but withering stage is affected; 2) In the whole growth process of tulip flowers, there were significant relationships between the growth of different florescence tulips and different organs (root, bulb, stem, leaf and flower) and ($Stan_{GDD}$), including linear, quadratic, logistic curve, power, and logarithmic functions; 3) NRMSE of the length index class, area class, proportion class, weight class and SLA simulation model respectively were within the range of 3.40%~29.22%, 17.34%~26.44%, 19.92%~23.85%, 8.26%~24.66% and 9.71%, and RMSE respectively were within the range of 0.25~8.19 cm, 3.36~47.80 cm^2, 0.29~1.86, 0.26~9.58 g $plant^{-1}$ and 1.27 m^2 kg^{-1}. In general, the growth model of different organs had high simulation accuracy. This study will be helpful in quantifying the morphology of each organ and flowering stage in solar greenhouse by calculating ($Stan_{GDD}$).

Keywords
Tulipa gesneriana L., morphology, flowering period, simulation model, standardized growing degree days

Significance of this study

What is already known on this subject?

- Most of the studies on tulip growth are performed qualitatively, but few studies research on the growth model of bulb flowers, especially of tulips, based on environmental factors.
- The climatic conditions of different geographical latitudes are different, leading to differences in greenhouse types, cultivation and management pattern.

What are the new findings?

- The results of this study showed that the flowering period is not affected by the variety, but the withering period is affected. The growth of different organs simulation models had high simulation accuracy.

What is the expected impact on horticulture?

- This study will be helpful in quantifying the morphology of each organ and flowering stage in solar greenhouse. Through this process, the light and temperature resources in the greenhouse can be rationally utilized, and it is helping users to obtain the greatest economic benefits in production.

Introduction

Landscape is an integral part of our environment with great impacts on humans (Hatamian et al., 2018) in which tulip (*Tulipa gesneriana* L.) plays an important role in its decoration and beauty (Nelson et al., 2003; Geng et al., 2005). Tulip cultivation and production in the field and in the pots is often affected by factors, such as climate, soil, diseases, insect pests, pollution sources and operation methods, and these difficulties resulted in tulips not achieving their best ornamental effect as scheduled (Ramírez-Martínez et al., 2009; Liu, 2015). Tulip hydroponic cultivation is not only overcoming the deficiency of conventional cultivation and giving full play to its ornamental characteristics, but it is also a simple and feasible cultivation method (Abasi et al., 2015). Initially, Netherlands produces approximately 0.8% of its tulips through greenhouse hydroponics, but by the early 2000s, that proportion has risen to 40% (Cerveny and Miller, 2010; Abasi et al., 2016). In tulips (Khan et al., 2006), similar to many other plants and crops, the growth is significantly influenced by medium available minerals or application of chemical or organic fertilizers (Souri and Naiji, 2018; Aghaye Noroozlo et al., 2019; Souri and Bakhtiarizade, 2019), and the results provide a theoretical reference that sets the ratio of fertilizer elements for obtaining better flower and bulb production. However, the influence of environmental factors

on the growth indicators of tulip organs is less quantitatively considered. Some results indicate that two important factors that could affect yields are sowing period and growing degree day (GDD) (Sacks and Kucharik, 2011). Accumulated temperature theory is mostly applied to field crops, such as corn and soybeans, and it would be a better method to simulate the development period for flower when only temperature is considered as the dominant meteorological factor (Li et al., 2011). However, due to differences in variety characteristics and too small parameters, it is necessary to standardize GDD to improve the accuracy of the model. The growth habits of the main cultivars under different climatic conditions and cultural practices are recorded and analysed (Zhang et al., 2009). However, the relationship between organ morphology and environment has not been thoroughly studied.

In general, the research on the growth analysis of the main organs of tulips still have the following deficiencies: (1) Most of the studies on tulip growth are performed qualitatively, mainly exploring the relationship between the growth indicators and the number of days after sowing. At the same time, mathematical models between tulip growth and environment factors, mainly air temperature, need to be established. Moreover, due to the differences in florescence characteristics, there is little significance to directly measuring GDD, which needs to be standardized. Finally, this study can achieve the goal of optimizing planting varieties, planting methods and planting period of tulips. (2) On the one hand, few studies research on growth model of bulb flowers, especially of tulips, based on environmental factors. On the other hand, the climatic conditions of different geographical latitudes are different, which are leading to differences in greenhouse types; the cultivation and management pattern of tulip are different. It is necessary to construct a universal growth model driven by environmental factors. (3) Most studies have relatively few indicators to evaluate tulip growth on the emerging of hydroponics methods, without water stress.

Materials and methods

Experimental material

The experimental location was set in No. B2 solar greenhouse base of Yangzhen International Flower Harbor, Shunyi district, Beijing, China. Six popular cultivars of tulip were selected for the study. These cultivars were 'Pink Impression (PI)' (a pink, early blossoming (EB) Darwin strain cultivar), 'Lalibela (LA)' (a red, middle blossoming (MB) Darwin strain cultivar), 'Huge Pink (HP)' (a pink, middle blossoming (MB) Darwin strain cultivar), 'Daydream (D)' (an orange, middle blossoming (MB) Darwin strain cultivar), 'Esmee (E)' (a red, late blossoming (LB) Darwin strain cultivar), 'Queen of Night (AW)' (a purple, very late blossoming (VB) Single Late Flowering strain cultivar).

The experiment was conducted using soilless hydroponic boxes, of which the width was 38.0 cm, the length 57.0 cm, and the height 17.5 cm. The greenhouse would take measures to cool down when the temperature exceeded 40°C. Experiment I: The experiment adopted a random block design, and was planted in cold storage on May 1st, 2016 and was moved into the greenhouse on June 15th, 2016. Two varieties ('Huge Pink' and 'Lalibela') with a density of 388 plants m^{-2} and three replicates were used. Experiment II: The experiment used a random block design from October 2016 to April 2017, growing four varieties ('Pink Impression', 'Daydream', 'Esmee' and 'Queen of Night') with a density of 388 plants m^{-2}, and three replicates were used. The experiment was carried out on three sowing dates: early planting (EP) done in cold storage on December 19th, 2016 and plants were moved into the greenhouse on February 3rd, 2017. Medium planting (MP) done in cold storage on December 29th, 2016 and plants were moved into the greenhouse on February 13th, 2017. Late planting (LP) done in cold storage on January 8th, 2017 and plants were moved into the greenhouse on February 23rd, 2017.

The microclimate observation in the greenhouse used a microclimate observer (Apresys, American Apresys (Shanghai) Co., Ltd.), which automatically recorded meteorological data of air temperature and air humidity in the greenhouse every 10 minutes. Data acquisition methods and measurement tools for different organ measurements and calculation items were shown in Table 1. The length index class, including the length and width of flower ($Length_{flower}$ and $Width_{flower}$), length and maximum width of leaf ($Length_{leaf}$ and $Width_{leaf}$), length and diameter of stem ($Length_{stem}$ and

Table 1. Data acquisition methods and measurement tools for measurements and calculation items of the different plant organs, including bulb, root, leaf, stem, and flower.

Organs	Measuring items	Expression	Measuring tool	Remarks
Leaf	Leaf area	LA	Grid paper	Number of grid method (Garnier et al., 2010)
	Leaf area index	LAI	Algorithm	LAI = LA * d/10.000 (Korhonen et al., 2017), where d is plant density (388 plants m^{-2})
	Specific leaf area	SLA	Algorithm	$SLA = LA/W_{dry_leaf}$ (Greenwood et al., 2017)
Stem	Distance of node spacing	$Distance_{stem}$	Vernier calliper	
	Plant height	H	Straightedge	
	Plant height uniformity	U_{height}	Algorithm	$U_{height} = 1/CV_{height}$, where CV_{height} is variable coefficient of plant height
	Moisture content of stem	OW_{stem}	Algorithm	$OW_{stem} = (W_{fresh_stem} - W_{dry_stem}) / W_{fresh_stem} \times 100\%$ (Brodribb and McAdam, 2017)
Weight	Dry weight of the whole plant	W_{dry_plant}	Algorithm	$W_{dry_plant} = W_{dry_overground} + W_{dry_underground}$
	Dry root/shoot ratio	R/S_{dry}	Algorithm	$R/S_{dry} = \frac{W_{dry_underground}}{W_{dry_overground}}$ (Li et al., 2018)
	Fresh weight of the whole plant	W_{fresh_plant}	Algorithm	$W_{fresh_plant} = W_{fresh_overground} + W_{fresh_underground}$
	Fresh root/shoot ratio	R/S_{fresh}	Algorithm	$R/S_{fresh} = \frac{W_{fresh_underground}}{W_{fresh_overground}}$

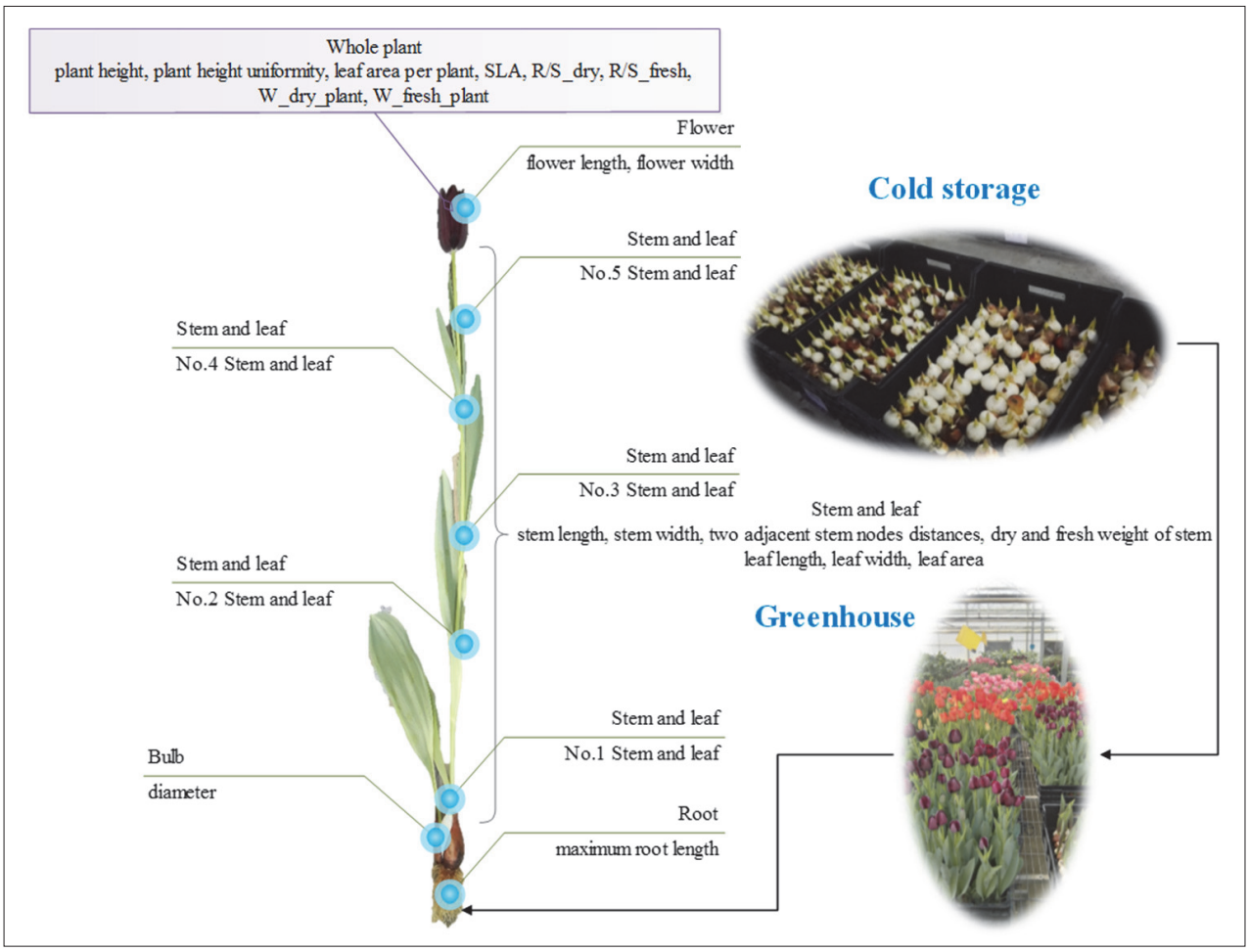


FIGURE 1. The specific position of growth indicators of the different plant organs, including bulb, root, leaf, stem, and flower.

$Width_{stem}$), diameter of bulb ($Diameter_{bulb}$) and maximum length of root ($Length_{root}$). The weight index class, including the fresh and dry weight of different organs (W_{fresh_organ} and W_{dry_organ}). The specific measurement position was shown in Figure 1.

GDD was calculated using formula (1) and formula (2), and the standardized growing degree days ($Stan_{GDD}$) was obtained using formula (3).

$$GDD_i = \sum_{i=0}^{M} (Tdi - Tb) \quad (1)$$

$$Tdi = \begin{cases} Tb, & Tdi < Tb \\ Tdi, & Tb \le Tdi \le Tm \\ Tm, & Tdi > Tm \end{cases} \quad (2)$$

$$Stan_{GDD} = \frac{GDD_i}{GDD_M} \quad (3)$$

where I = 0,1..., M, represented the growing days from sowing; 0 represented the sowing date; M represented the number of days for the whole development of the plant until harvest. *Tdi* was the daily average temperature, °C. *Tb* was the lower limit of biological temperature, set at 4°C. *Tm* was the biological upper limit temperature, set at 40°C (Xu et al., 2006; Kim et al., 2007; Li et al., 2011). GDD_i was the growing degree on day i (°C d), and GDD_m was the total growing degree days at the whole development stage (°C d).

Statistical variables of model validation

Experiment data segmented into learning and validation sets, and the data sets are independent of each other. Learning set: experimental data of EP and LP in "Experiment II". Validation set: experimental data of "Experiment I" and MP in "Experiment II". Variance analysis and function regres-

TABLE 2. The GDD at each reproductive stage of different varieties at different sowing periods.

Variety	Sowing – Rooting	Rooting – Leaf-expansion	Leaf-expansion – Squaring	Squaring – Flowering	Flowering – Full-bloom	Full-bloom – End of the flowering	End of the flowering – Withering	Sum of growth stages
EB	2.26	116.50	97.33	37.72	47.60	141.13	172.25	614.79
MB	3.74	136.53	81.12	42.94	64.69	118.12	210.21	657.35
LB	2.42	137.85	113.54	37.33	32.72	161.69	286.24	771.79
VB	4.56	173.04	113.38	32.70	63.78	132.16	385.66	905.28
Average	3.25	140.98	101.34	37.67	52.2	138.28	263.59	737.31

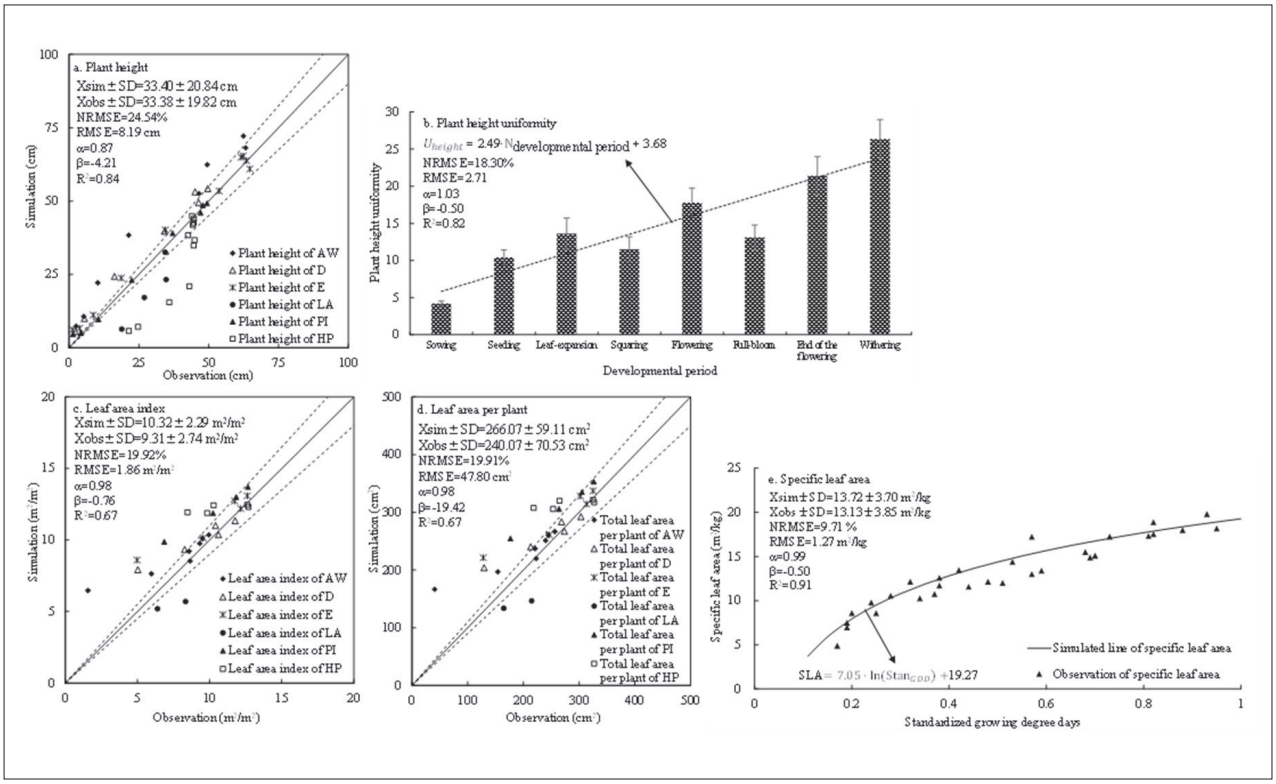


FIGURE 2. Verification of whole plant morphology indices (including the plant height, leaf area index and leaf area per plant) with standardized growing degree days of different varieties, and the tendency between plant height uniformity and the development period and between SLA and standardized growing degree days of different varieties.

TABLE 3. Parameters list of dry and fresh weight in simulation model.

Organs	Varieties	Fitted equation	Param. a	Param. b	Param. c	NRMSE (%)	RMSE (g plant^{-1})
Fresh weight of overground part	EB	$W_{fresh_overground} = \frac{c}{(1+e^{(a\cdot Stan_{GDD}+b)})}$	-13.77	3.77	43.0	12.67	2.10
	MB		-13.49	4.27	43.0	12.00	2.05
	LB		-12.94	3.86	57.6	27.05	7.00
	VB		-14.85	4.12	42.6	16.98	3.22
Fresh weight of underground part	EB	$W_{fresh_underground} = \frac{c}{(1+e^{(a\cdot Stan_{GDD}+b)})}$	-2.08	-1.18	45.4	15.48	5.77
	MB		-3.58	-1.56	39.6	13.35	4.62
	LB		-3.10	-0.57	67.5	10.57	6.07
	VB		-2.76	-0.65	44.6	11.01	4.01
Fresh weight of the whole plant	EB	$W_{fresh_plant} = \frac{c}{(1+e^{(a\cdot Stan_{GDD}+b)})}$	-8.73	0.69	83.5	15.27	8.12
	MB		-4.69	0.49	82.4	9.05	4.88
	LB		-3.03	0.06	119.3	17.01	14.40
	VB		-6.75	0.68	82.0	10.23	5.19
Dry weight of overground part	EB	$W_{dry_overground} = \frac{c}{(1+e^{(a\cdot Stan_{GDD}+b)})}$	-11.27	2.98	3.8	21.27	0.36
	MB		-11.36	3.25	3.5	7.25	0.17
	LB		-11.63	3.44	5.2	17.26	0.40
	VB		-13.10	3.47	4.3	17.71	0.38
Dry weight of underground part	EB	$W_{dry_underground} = a\cdot Stan_{GDD}^{\ 2} + b\cdot Stan_{GDD} + c$	1.75	-2.48	3.75	10.62	0.35
	MB		3.70	-4.07	3.53	7.30	0.21
	LB		4.71	-5.02	6.20	7.88	0.45
	VB		3.26	-4.16	4.21	6.21	0.22
Dry weight of the whole plant	EB	$W_{dry_plant} = \frac{c}{(1+e^{(a\cdot Stan_{GDD}+b)})}$	-4.99	-0.15	7.0	6.53	0.33
	MB		-2.55	-0.33	6.3	4.24	0.20
	LB		-1.73	-0.80	10.2	9.61	0.80
	VB		-5.04	-0.25	7.4	7.80	0.44

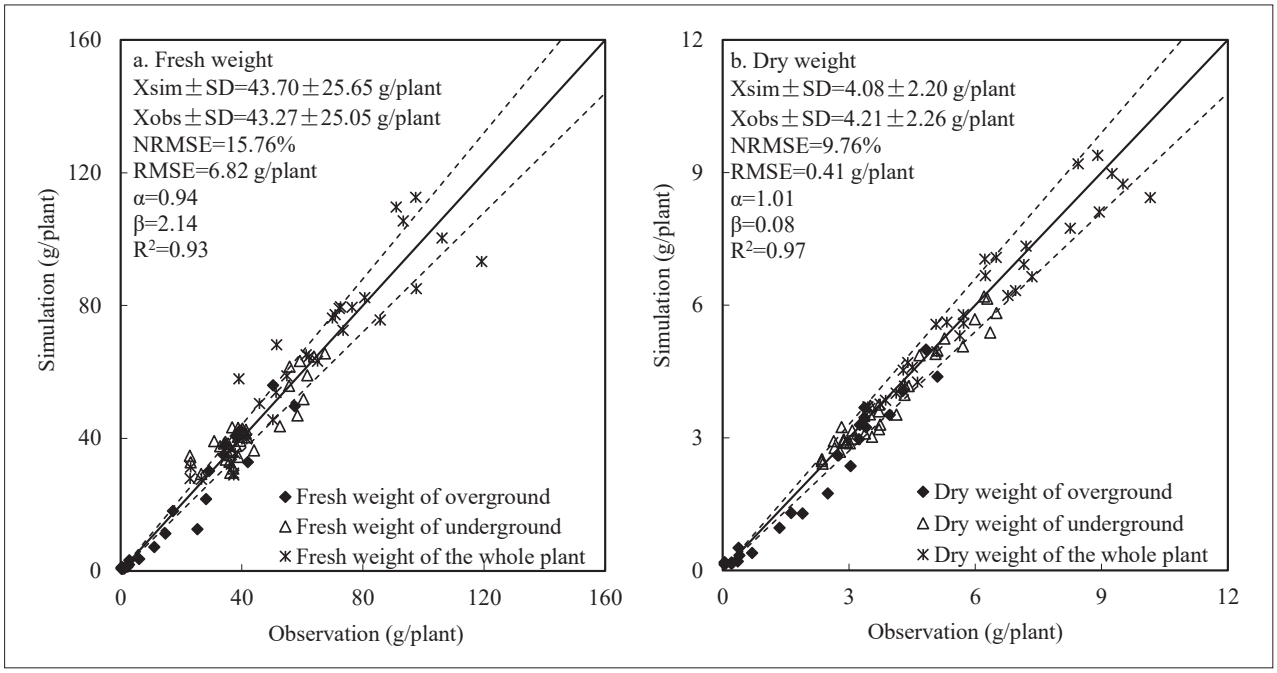


Figure 3. Verification of dry and fresh matter accumulation with standardized growing degree days of different position and varieties.

sion analysis were performed with the experimental data using Excel 5.0. The accuracy of the model is reflected by mean value $\overline{X}$, standard deviation SD, linear regression coefficient α, intercept β, coefficient R^2, root mean square error (RMSE, formula (4)) and normalized root mean square error (NRMSE, formula (5)) (Cheng et al., 2020). RMSE and NRMSE are used to measure the deviation between the observed value and the measured values, reflecting the precision of the model. Accuracy values are calculated as follows:

$$\mathrm{RMSE} = \sqrt{\frac{\sum (\mathrm{Xobs} - \mathrm{Xsim})^2}{\mathrm{n}}} \quad (4)$$

$$\mathrm{nRMSE} = 100 \times \frac{\mathrm{RMSE}}{\overline{\mathrm{Xobs}}} \quad (5)$$

Results

Whole growth analysis

On the basis of Table 2, the amount of GDD accumulated during the flowering period of different varieties was similar, which was within the range of 225.75°C d ~ 231.74°C d. For the amount of GDD accumulated during the wilting stage of different varieties was significant different, ranked by VB (385.66°C d) > LB (286.24°C d) > MB (210.21°C d) > EB (172.25°C d).

The tendency of plant height (H), leaf area per plant (LA_{plant}) and leaf area index (LAI) for the different varieties of tulips revealed a Logistic curve function with ($Stan_{GDD}$) (formula (6) ~ formula (8)). The tendency of plant height uniformity (U_{height}) of tulips revealed a linear function with ($Stan_{GDD}$) (formula (9)). The tendency of specific leaf area (SLA) for different varieties of tulips revealed a logarithmic curve function with ($Stan_{GDD}$) (formula (10)).

$$\mathrm{H} = \frac{H_{\max}}{(1+e^{(a \cdot \mathrm{Stan}_{GDD}+b)})} \quad (6)$$

where a was -8.64, b was 2.41, and H_{max} was the maximum plant height that it was related to varietal characteristics, and plant height was ranked by AW (72.4 cm) >E (65.5 cm) >D (54.7 cm) >LA (49.9 cm) >PI (49.5 cm) >HP (45.0 cm).

$$LA_{plant} = \frac{LA_{\mathrm{plant_max}}}{(1+e^{(\alpha \cdot \mathrm{Stan}_{GDD}+b)})} \quad (7)$$

$$\mathrm{LAI} = LA_{plant} \cdot \frac{\mathrm{d}}{10000} \quad (8)$$

where a was -4.42, b was 0.34 (formula (7), d was the planting density, 338 plants m^{-2} (formula (8)), and LA_{plant} was the maximum leaf area per plant that related to varietal characteristics, which was ranked by PI (372.9 cm^2) >E (349.7 cm^2) >HP (327.1 cm^2) >D (303.3 cm^2) >AW (227.2 cm^2).

$$U_{height} = \mathrm{a} \cdot \mathrm{N}_{\mathrm{developmental\ period}} + \mathrm{b} \quad (9)$$

where a was 2.49, b was 3.68, $N_{developmental\ period}$ = 1 to 8, which represents the development period of tulip growth, 1 represented sowing period, and 8 represented withering period.

$$\mathrm{SLA} = a \cdot \ln(\mathrm{Stan}_{GDD}) + \mathrm{b} \quad (10)$$

where a was 7.05, b was 19.27.

In the light of Figure 2, the accuracy of H simulation model was medium (Figure 2a), the accuracy of U_{height}, LAI and LA_{plant} simulation model was high (Figure 2b–d), the accuracy of the SLA simulation model was extremely high (Figure 2e).

In Table 3, the tendency of dry and fresh weight of aboveground, underground and the whole plant revealed a logistic curve function with $Stan_{GDD}$, and the tendency of underground dry weight revealed a quadratic function with $Stan_{GDD}$, which went down first and then went up. The maximum value of dry and fresh weight of the whole plant for different varieties was ranked by LB > EB > MB > VB. $Stan_{GDD}$ of the maximum of the whole plant dry weight for the different varieties sequence was EB (0.71) > VB (0.64) > MB (0.55) > LB (0.53). NRMSE of fresh weight for different cultivars had a range from 9.05% to 27.05%, and RMSE ranged from 2.05 to 14.40 g $plant^{-1}$. NRMSE of dry weight for different cultivars ranged from 4.24% to 21.27%, and RMSE ranged from 0.17

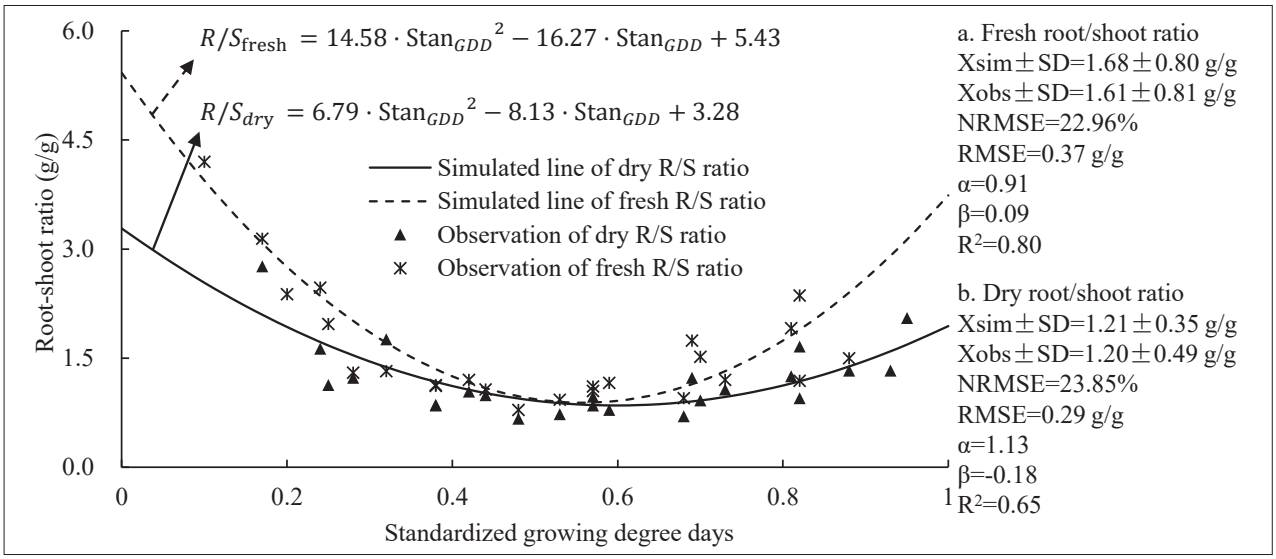


FIGURE 4. The tendency of dry and fresh of R/S with standardized growing degree days in different varieties.

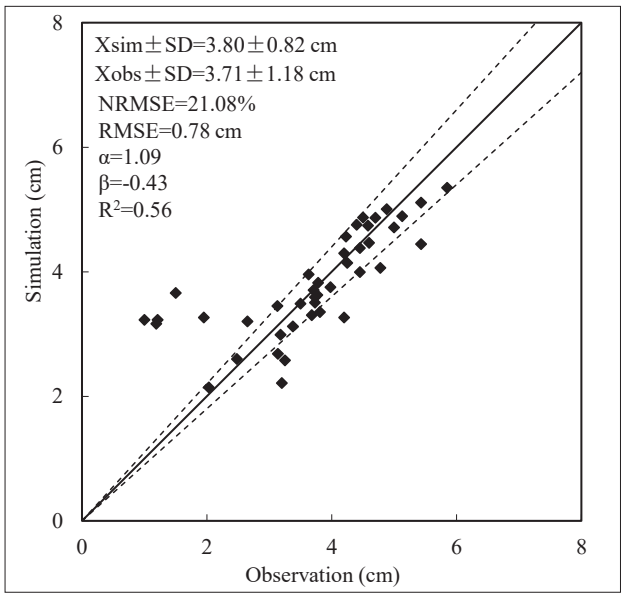


FIGURE 5. Verification of maximum root length with standardized growing degree days of different varieties.

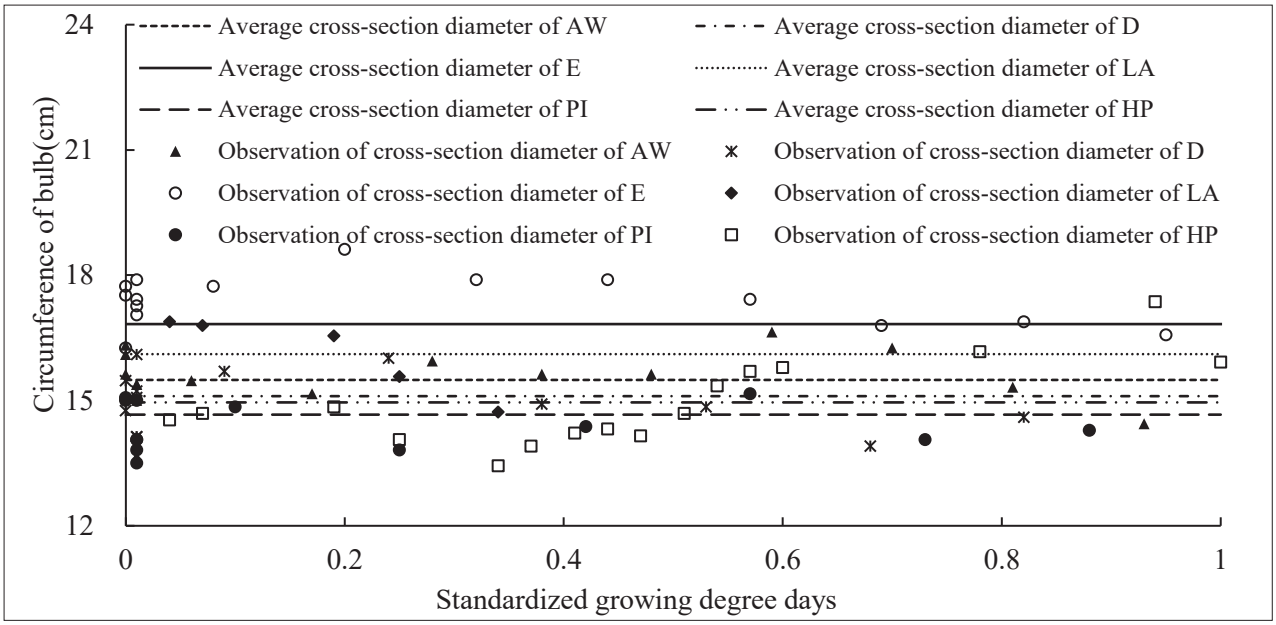


FIGURE 6. Tendency of diameter of bulb with standardized growing degree days for the different varieties.

Table 4. Parameters list of morphology indices of different stem positions (including the stem length, width and distance) in the simulation model.

Morphology index	Indicators	Parameter a	Parameter b	Parameter c	$-\frac{b}{2a}$
Stem length	No. 1 stem	1.09	-2.82	–	–
	No. 2 stem	-0.16	-2.51	–	–
	No. 3 stem	-1.18	-1.92	–	–
	No. 4 stem	42.37	0.53	–	–
Stem width	No. 1 stem	-7.39	6.36	8.4	0.43
	No. 2 stem	-10.46	10.39	5.49	0.5
	No. 3 stem	-11.42	11.55	3.78	0.51
	No. 4 stem	-14.75	15.26	1.83	0.52
Stem distance	No. 1~No. 2 stem	-0.62	-2.08	–	–
	No. 2~No. 3 stem	-1.08	-1.67	–	–

to 0.80 g plant^{-1}. In conclusion, the model simulation accuracy of the change of dry and fresh matter accumulation with $Stan_{GDD}$ of different organs and varieties was high. In Figure 3, the accuracy of the fresh matter accumulation simulation model was high, and the accuracy of the dry matter accumulation simulation model was extremely high.

The tendency of fresh and dry R/S for different varieties of tulips revealed a quadratic curve function with $Stan_{GDD}$ (formula (11) ~ formula (12)).

$$R/S_{fresh} = a \cdot Stan_{GDD}{}^2 + b \cdot Stan_{GDD} + c \quad (11)$$

$$R/S_{dry} = a \cdot Stan_{GDD}{}^2 + b \cdot Stan_{GDD} + c \quad (12)$$

where a, b and c are shown in Figure 4. According to the value of –(b/2a) , the $Stan_{GDD}$ of the maximum R/S of dry and fresh weights for different varieties sequence was R/S_{dry} (0.60) > R/S_{fresh} (0.56). As seen from Figure 4, the accuracy of the dry and fresh R/S simulation models were medium.

Root growth analysis

The tendency of the maximum root length of the different varieties of tulips revealed a Logistic curve function with $Stan_{GDD}$ (formula (13)).

$$Length_{root} = \frac{Length_{root_max}}{(1+e^{(a \cdot Stan_{GDD}+b)})} \quad (13)$$

where a was -3.12, b was -0.4917, and $Length_{root\ max}$ was the maximum root length that related to varietal characteristics, with the maximum root length ranked by E (5.9 cm) >AW = PI (5.2 cm) > D (5.1 cm) > HP (4.0 cm) > LA (3.3 cm). According to Figure 5, the accuracy of the $Length_{root}$ simulation model was medium.

Bulb growth analysis

In the whole growth and development process of tulips, the circumference of the bulb was maintained within a certain range (formula (14)), which related to the biological characteristics of the different varieties, as shown in Figure 6.

$$Circumference_{bulb} = Circumference_{bulb_average} \quad (14)$$

The average circumference of the bulb was ranked by E (16.83 cm) > LA (16.11 cm) > AW (15.49 cm) > D (15.10 cm) > HP (14.95 cm) > PI (14.66 cm). The circumference of the bulb was greater than 12+ cm to meet production standards.

Stem growth analysis

The tendency from No. 1 to No. 3 stems length of the different varieties of tulips revealed a Logistic curve function with $Stan_{GDD}$, from No. 4 to No. 5 stems length of different varieties of tulips revealed a power function with $Stan_{GDD}$, and No. 6 stem length of different varieties of tulips revealed a linear function over $Stan_{GDD}$ (formula (15)).

$$Length_{stem} = \begin{cases} \frac{Length_{stem_max}}{(1+e^{(a \cdot Stan_{GDD}+b)})}, n \le 3 \\ a \cdot Stan_{GDD}^{b}, 5 \ge n \ge 4 \\ a \cdot Stan_{GDD} + b, n = 6 \end{cases} \quad (15)$$

The tendency of the stem width for different positions and varieties of tulips revealed a quadratic function with $Stan_{GDD}$, which went up first and then went down (formula (16)).

$$Width_{stem} = a \cdot Stan_{GDD}{}^2 + b \cdot Stan_{GDD} + c \quad (16)$$

The tendency of two adjacent distances of stem for different positions and varieties of tulips revealed a Logistic curve function with $Stan_{GDD}$ (formula (17)).

$$Distance_{No.n\sim No.n+1_{stem}} = \frac{Distance_{No.n\sim No.n+1_stem_max}}{(1+e^{(a \cdot Stan_{GDD}+b)})} \quad (n \le 2) \quad (17)$$

where n was the number of stems in order from bottom to top, and $Length_{stem_max}$ was the maximum stem length at different positions and $Distance_{No.n\sim No.n+1_stem_max}$ was the maximum stem length between two adjacent distances of stem, which related to the varietal characteristics. Where a, b of $Length_{stem}$ and $Width_{stem}$ were shown in Table 4, $Length_{stem_max}$ of No. 1 stem was ranked by D (13.4 cm) > E (12.0 cm) > AW (10.1 cm) > LA (9.7 cm) > HP (8.7 cm) > PI (7.3 cm). $Length_{stem_max}$ of No. 2 stem was ranked by AW (22.3 cm) > E (21.7 cm) > D (21.5 cm) > PI (16.0 cm) > HP (15.0 cm) > LA (14.8 cm). $Length_{stem_max}$ of No. 3 stem was ranked by AW (32.4 cm) >E (32.0 cm) > D (30.4 cm) > PI (24.7 cm) > HP (21.7 cm) > LA (18.0 cm). According to the value of –(b/2a), the maximum $Width_{stem}$ of different positions appeared in the middle of the whole developmental stage (0.43~0.53). $Distance_{No.1\sim No.2_stem_max}$ was ranked by AW (12.3 cm) > E 9.7 cm) > PI (9.5 cm) > D (8.7 cm) > HP (7.0 cm) > LA (4.9 cm). $Distance_{No.2\sim No.3_stem_max}$ was ranked by E (11.7 cm) > AW (10.2 cm) > PI (9.6 cm) > D (9.2 cm) > HP (6.3 cm) > LA (4.1 cm).

Table 5. Statistics for validation of stem morphology indices (including the stem length, width and distance) of different positions and varieties.

Morphology index	Indicators	$\bar{X}_{sim}$ ± SD	$\bar{X}_{obs}$ ± SD	α	β	R^2	RMSE	NRMSE (%)
Stem length	No. 1 stem	8.88±1.78 cm	8.64±1.85 cm	0.88	0.83	0.71	1.03 cm	11.91
	No. 2 stem	17.03±3.13 cm	16.58±2.48 cm	0.71	4.47	0.80	1.48 cm	8.90
	No. 3 stem	23.61±4.69 cm	24.18±4.13 cm	0.56	10.89	0.41	3.75 cm	15.53
	No. 4 stem	29.54±6.64 cm	29.99±8.05 cm	0.93	2.49	0.59	5.10 cm	17.01
	No. 5 stem	31.43±6.29 cm	31.51±5.52 cm	0.58	13.42	0.43	4.83 cm	15.34
	No. 6 stem	52.92±10.24 cm	50.70±8.37 cm	0.76	10.44	0.86	4.37 cm	8.63
Stem width	No. 1 stem	9.29±0.50 mm	9.24±1.85 mm	0.96	0.29	0.70	0.31 mm	3.40
	No. 2 stem	7.62±0.58 mm	7.62±0.70 mm	-0.21	1.03	0.72	0.36 mm	4.78
	No. 3 stem	6.22±0.59 mm	6.29±0.69 mm	-0.18	1.04	0.78	0.33 mm	5.17
	No. 4 stem	5.16±0.79 mm	5.34±0.99 mm	1.04	0	0.68	0.58 mm	10.89
	No. 5 stem	4.54±0.81 mm	4.66±1.03 mm	1.08	-0.23	0.71	0.56 mm	11.93
	No. 6 stem	4.28±1.12 mm	4.36±1.31 mm	1.10	-0.36	0.88	0.45 mm	10.24
Stem distance	No. 1 ~ No. 2 stem	9.67±2.20 cm	8.08±1.97 cm	0.85	-0.18	0.92	1.71 cm	21.15
	No. 2 ~ No. 3 stem	9.48±2.45 cm	7.70±2.20 cm	0.84	-0.26	0.87	1.99 cm	25.81

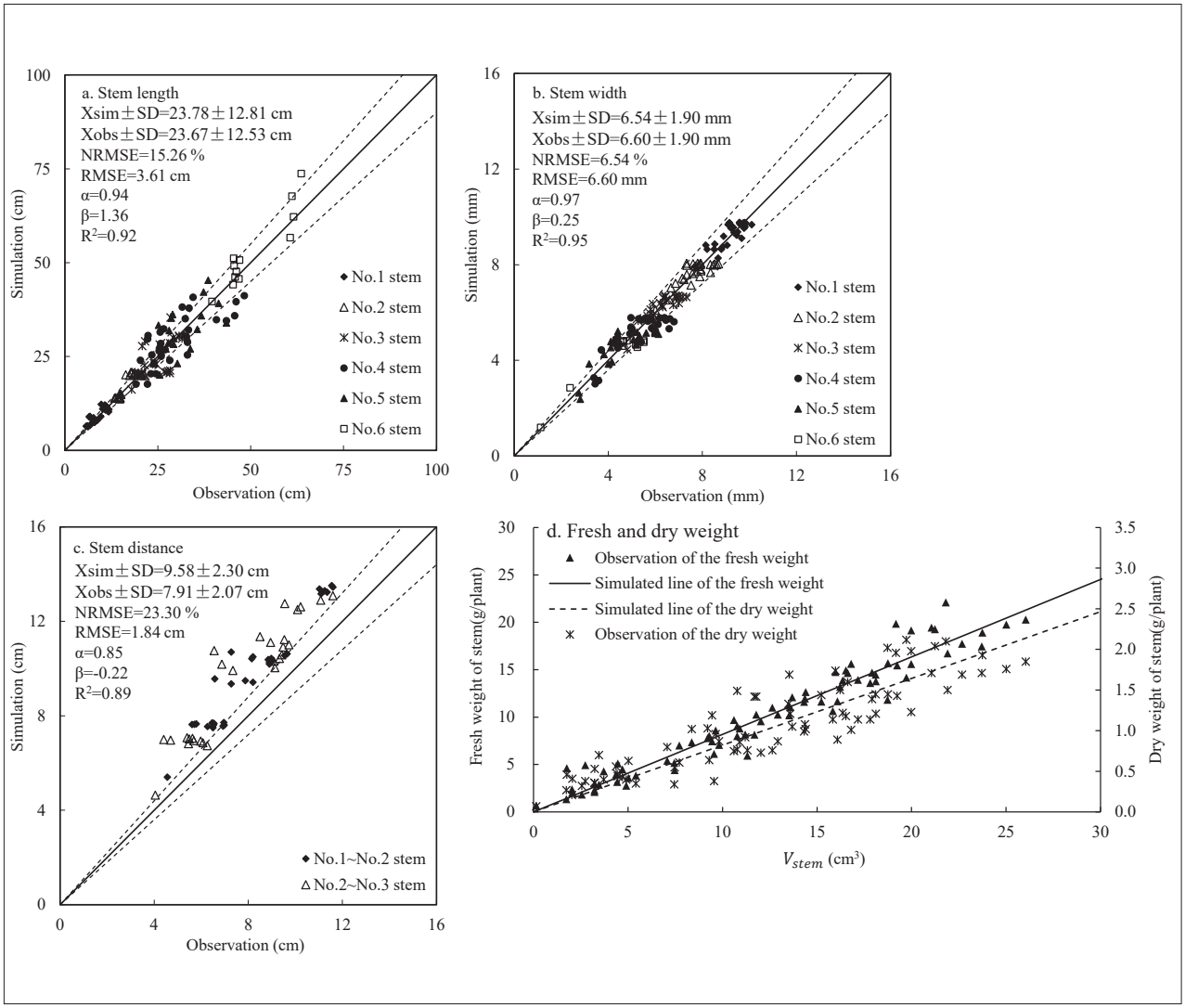


Figure 7. Verification of stem morphology indices (including the stem length, width and distance) with standardized growing degree days of different positions and varieties, and the tendency between fresh and dry weight and stem with V_{stem}.

The dry and fresh weight of stems revealed a linear function with

$$\sum_{i=0}^{n} 3.14 * Length_{stem} * (\frac{Width_{stem}}{20})^2,$$

which was based on the morphology mathematical formula (formula (18) ~ formula (19)). OW_{stem} was the moisture content of stem (formula (20)).

$$W_{fresh_{stem}} = a \cdot V_{stem} = a \cdot 3.14 \cdot Length_{stem} \cdot (\frac{Width_{stem}}{20})^2 \quad (18)$$

$$W_{dry_{stem}} = b \cdot V_{stem} = b \cdot 3.14 \cdot Length_{stem} \cdot (\frac{Width_{stem}}{20})^2 \quad (19)$$

$$OW_{stem} = \frac{W_{fresh_{stem}} - W_{dry_{stem}}}{W_{fresh_{stem}}} \cdot 100\% = (a - b)/a \cdot 100\% = 89.95\% \quad (20)$$

where a was 0.82 (formula (18)), b was 0.08 (formula (19)). The formula expressed the relationship between the volume and fresh and dry weight of the stem, and on the assumption that the stem was a cylinder, according to the formula of volume calculation, for which base area was:

$$3.14 \cdot (\frac{Width_{stem}}{20})^2.$$

In Table 5, the accuracy of No. 2 and No. 6 $Length_{stem}$ simulation models were extremely high and others were high. The accuracy of $Length_{stem}$ of different position simulation models ranked by No. 6 > No. 2 > No. 1 > No. 5 > No. 3 > No. 4. The accuracy of No. 1~No. 3 $Width_{stem}$ simulation models were extremely high and the accuracy of No. 4~No. 6 $Width_{stem}$ simulation models were high. The accuracy of the simulation model of $Width_{stem}$ at different positions was ranked No. 1 > No. 2 > No. 3 > No. 6 > No. 4 > No. 5. The accuracy of the $Distance_{No.n\sim No.n+1_stem}$ simulation model was medium. In the light of Figure 7, the accuracy of $Length_{stem}$ and W_{fresh_stem} simulation model was high, the accuracy of $Width_{stem}$ simulation model was extremely high, and the accuracy of $Distance_{No.n\sim No.n+1_stem}$ and W_{dry_stem} simulation model was medium.

Leaf growth analysis

The tendency of leaf length (formula (21)), leaf width (formula (22)) and leaf area (formula (23)) at different positions and varieties of tulips revealed a Logistic curve function with $Stan_{GDD}$.

$$Length_{leaf} = \frac{Length_{leaf_max}}{(1+e^{(a \cdot Stan_{GDD}+b)})} \quad (21)$$

$$Width_{leaf} = \frac{Width_{leaf_max}}{(1+e^{(a \cdot Stan_{GDD}+b)})} \quad (22)$$

$$LA_{leaf} = \frac{LA_{leaf_max}}{(1+e^{(a \cdot Stan_{GDD}+b)})} \quad (23)$$

The tendency of leaf area revealed a linear function with $Length_{leaf}$ * $Width_{leaf}$, which was based on the morphology mathematical formula (formula (24)).

$$LA = a \cdot Length_{leaf} \cdot Width_{leaf} \quad (24)$$

where $Length_{leaf_max}$ and $Width_{leaf_max}$ were the maximum leaf length and width for different leaf positions, and LA_{leaf_max} was the maximum leaf area for different leaf positions, which related to varietal characteristics. Where a, b of $Length_{leaf}$ and $Width_{leaf}$ were shown in Table 6, $Length_{leaf_max}$ of No. 1 leaf was ranked by HP (30.6 cm) > PI (29.7 cm) > LA (25.3 cm) > E (24.0 cm) > D (22.8 cm) > AW (21.9 cm). $Length_{leaf_max}$ of No. 2 leaf was ranked by PI (27.3 cm) > HP (27.2 cm) > E (22.2 cm) > D (20.6 cm) > LA (19.6 cm) > AW (19.4 cm).

Table 6. Parameters list of morphology indices of different leaf positions (including the leaf length, width and area) in simulation model.

Morphology index	Parameters	No. 1 leaf	No. 2 leaf	No. 3 leaf	No. 4 leaf	No. 5 leaf
Leaf length	Parameter a	-3.90	-4.52	-4.08	-2.99	-4.50
	Parameter b	-0.58	-0.28	-0.03	-0.82	–
Leaf width	Parameter a	-0.85	-1.40	-2.21	-1.28	-1.45
	Parameter b	-2.29	-1.51	-0.90	-1.11	-1.16
Leaf area	Parameter a	-2.39	-2.99	-3.81	-2.00	-3.56
	Parameter b	-0.92	-0.35	0.32	-0.51	0.28

Table 7. Parameters list of leaf area with $Length_{leaf} \cdot Width_{leaf}$ for different leaf positions in different periods.

Indices		Fitted equation	Parameter a	R^2
Leaves position	Leaf 1	$LA = a \cdot Length_{leaf} \cdot Width_{leaf}$	0.75	0.94
	Leaf 2		0.72	0.95
	Leaf 3		0.67	0.96
	Leaf 4		0.63	0.91
	Leaf 5		0.62	0.67
Development stage	Squaring period to flowering period stage	$LA = a \cdot Length_{leaf} \cdot Width_{leaf}$	0.72	0.98
	Flowering period to full-bloom stage		0.72	0.98
	Full-bloom stage to end of the flowering		0.74	0.99
	End of the flowering to withering period		0.73	0.98
	The whole development period		0.73	0.99

Table 8. Statistics for validation of stem morphology indices (including the leaf length, width and area) for different positions and varieties.

Morphology index	Indicators	$\bar{X}_{sim}$ ± SD	$\bar{X}_{obs}$ ± SD	α	β	R^2	RMSE	NRMSE (%)
Leaf length	No. 1 leaf	24.10±3.81 cm	23.40±5.14 cm	1.26	-7.03	0.87	2.17 cm	9.26
	No. 2 leaf	21.39±3.58 cm	20.87±4.24 cm	1.06	-1.70	0.79	1.98 cm	9.48
	No. 3 leaf	15.95±3.18 cm	15.85±4.16 cm	1.20	-3.27	0.84	1.76 cm	11.12
	No. 4 leaf	13.95±2.99 cm	13.69±3.69 cm	1.13	-2.05	0.83	1.55 cm	11.33
	No. 5 leaf	12.34±2.82 cm	12.18±3.74 cm	1.30	-3.85	0.96	1.12 cm	9.23
Leaf width	No. 1 leaf	7.04±1.29 cm	6.91±1.25 cm	0.87	0.78	0.81	0.59 cm	8.47
	No. 2 leaf	5.12±1.10 cm	4.98±1.02 cm	0.78	1.01	0.70	0.62 cm	12.39
	No. 3 leaf	3.55±0.51 cm	3.54±0.54 cm	0.87	0.44	0.69	0.30 cm	8.58
	No. 4 leaf	2.60±0.55 cm	2.56±0.43 cm	0.47	1.35	0.35	0.45 cm	17.57
	No. 5 leaf	1.97±0.11 cm	1.95±0.26 cm	0.66	0.64	0.08	0.25 cm	12.66
Leaf area	No. 1 leaf	128.64±25.91 cm^2	119.04±28.14 cm^2	0.78	18.37	0.52	22.18 cm^2	18.63
	No. 2 leaf	80.62±17.98 cm^2	75.30±19.09 cm^2	0.70	18.61	0.44	15.93 cm^2	21.16
	No. 3 leaf	38.13±9.35 cm^2	36.91±11.39 cm^2	1.01	-1.56	0.69	6.40 cm^2	17.34
	No. 4 leaf	23.05±5.62 cm^2	21.39±6.49 cm^2	0.68	5.63	0.35	5.66 cm^2	26.44
	No. 5 leaf	15.03±4.16 cm^2	14.21±6.13 cm^2	1.26	-4.69	0.73	3.36 cm^2	23.66

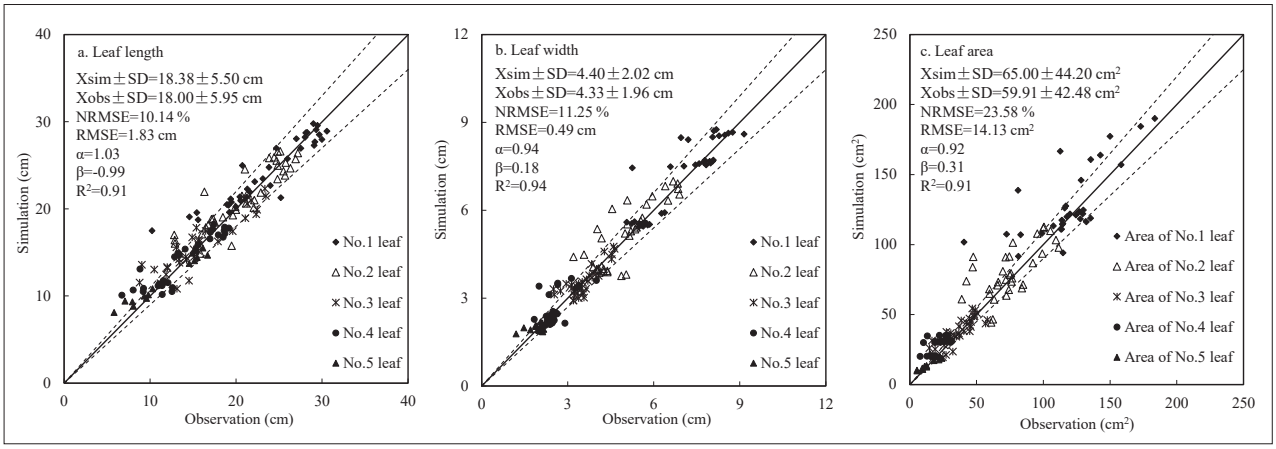


Figure 8. Verification of leaf morphology indices (including the leaf length, width, area and area index) with standardized growing degree days for different leaf positions and varieties.

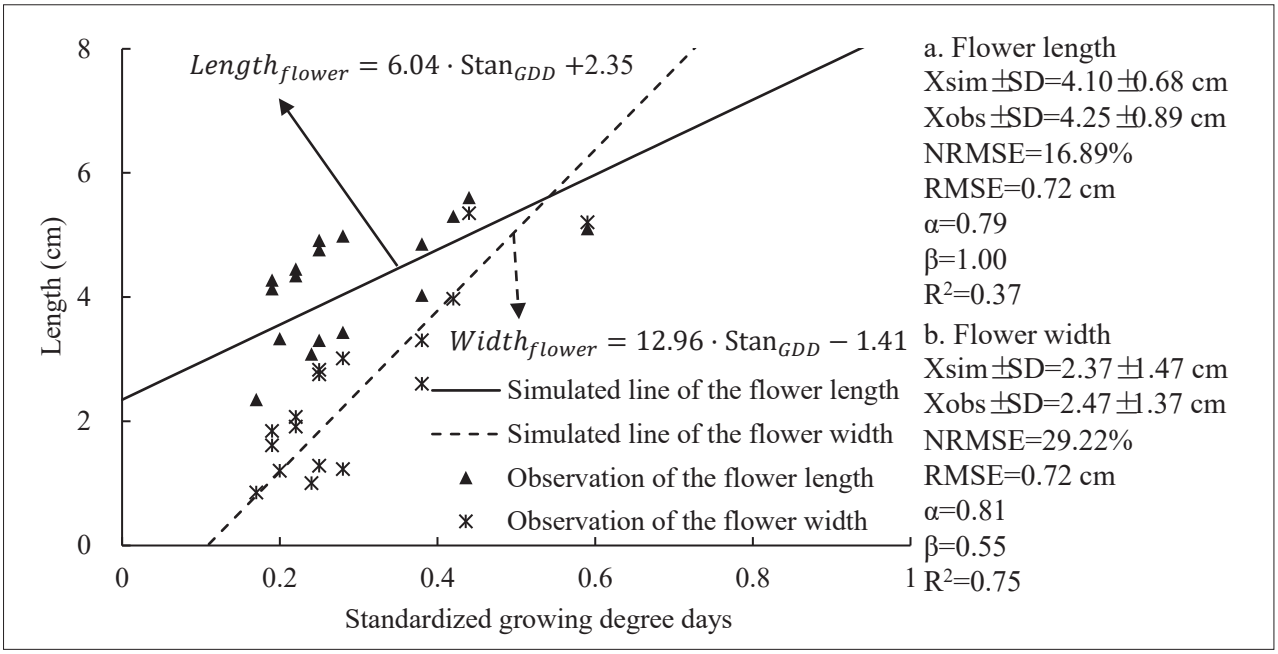


Figure 9. The tendency of flower length and flower width with standardized growing degree days for different varieties.

$Length_{leaf_max}$ of No. 3 leaf was ranked by HP (23.5 cm) > PI (18.3 cm) > E (16.8 cm) > D (15.7 cm) > AW (15.0 cm) > LA (14.6 cm). $Length_{leaf_max}$ of No. 4 leaf was ranked by HP (19.2 cm) > E (15.3 cm) > LA (12.7 cm) > D (12.2 cm) > AW (12.0 cm). $Length_{leaf_max}$ of No. 5 leaf was ranked by HP (16.7 cm) > D (11.1 cm) > AW (10.4 cm). $Width_{leaf_max}$ of No. 1 leaf was ranked by E (9.2 cm) > PI (9.1 cm) > D = AW (8.1 cm) > LA (6.4 cm) > HP (5.9 cm). $Width_{leaf_max}$ of No. 2 leaf was ranked by E (7.4 cm) > D (7.0 cm) > PI (6.2 cm) > AW (5.8 cm) > LA (5.1 cm) > HP (4.4 cm). $Width_{leaf_max}$ of No. 3 leaf was ranked by E (5.0 cm) > D (4.1 cm) > PI (4.0 cm) > AW (3.8 cm) > HP (3.7 cm) > LA (3.6 cm). $Width_{leaf_max}$ of No. 4 leaf was ranked by D (4.1 cm) > E (3.8 cm) > LA (3.0 cm) > AW (2.8 cm) > HP (2.6 cm). $Width_{leaf_max}$ of No. 5 leaf was ranked by AW (2.4 cm) > HP (2.2 cm) > D (2.1 cm). LA_{leaf_max} of No. 1 leaf was ranked by PI (203.3 cm^2) > E (173.1 cm^2) > HP (135.4 cm^2) > D (131.6 cm^2) > AW (128.9 cm^2) > LA (114.8 cm^2). LA_{leaf_max} of No. 2 leaf was ranked by PI (121.7 cm^2) > E (116.4 cm^2) > D (99.3 cm^2) > HP (84.9 cm^2) > AW (79.6 cm^2) > LA (62.2 cm^2). LA_{leaf_max} of No. 3 leaf was ranked by HP (58.1 cm^2) > E (51.8 cm^2) > PI (48.0 cm^2) > D (40.4 cm^2) > AW (37.2 cm^2) > LA (32.3 cm^2). LA_{leaf_max} of No. 4 leaf was ranked by E (35.3 cm^2) > HP (31.4 cm^2) > D (30.4 cm^2) > AW (20.5 cm^2) > LA (20.2 cm^2). LA_{leaf_max} of No. 5 leaf was ranked by HP (23.9 cm^2) > AW (14.5 cm^2) > D (13.8 cm^2). Where the leaf positions were increasing, the parameter a decreased gradually (Table 7). At different leaves position, parameter a was between 0.62 and 0.75 (formula (24)). At different development stage, there also was a good linear correlation, parameter a was between 0.72 and 0.74, which implied that the whole growth process for tulip was maintained within this range.

In Table 8, the accuracy of $Length_{leaf}$ for No. 3 and No. 4 simulation models were high and the others were extremely high. The accuracy of $Length_{leaf}$ for the different position simulation models were ranked No. 5 > No. 1 > No. 2 > No. 3 > No. 4. The accuracy of $Width_{leaf}$ of No. 1 and No. 3 simulation models were extremely high and the accuracy of the other models were high. The accuracy of $Width_{leaf}$ of different position simulation models ranked No. 1 > No. 3 > No. 2 > No. 5 > No. 4. The accuracy of LA_{leaf} for No. 1 and No. 3 simulation models was high and the accuracy of the others were medium. The accuracy of LA_{leaf} for the different position simulation models was ranked the same as leaf width. As seen from Figure 8, the accuracy of the $Length_{leaf}$ and $Width_{leaf}$ simulation model was high, and the accuracy of the LA_{leaf} simulation model was medium.

Flower growth analysis

The tendency of flower length (formula (25)) and flower width (formula (26)) for different varieties of tulips revealed a linear function with $Stan_{GDD}$.

$$Length_{flower} = a \cdot Stan_{GDD} + b \quad (25)$$

$$Width_{flower} = a \cdot Stan_{GDD} + b \quad (26)$$

where a was 6.04 and b was 2.35 (formula (25)), and a was 12.96 and b was -1.41 (formula (26)), parameter a illustrated that the growth rate of the flower width was faster than that of the flower length.

According to Figure 9, the observed values were dispersed out on both sides of the simulation line. The accuracy of the $Length_{flower}$ simulation model was high and the accuracy of the $Width_{flower}$ simulation model was medium.

Discussion

This study will be helpful in quantifying the morphology of each organ and flowering stage in solar greenhouse. On the one hand, there were many flower researches for field cultivation (Polder et al., 2014; Douglas et al., 2014; Jeung and Roh, 2014), but for the emerging method of hydroponic cultivation there were less. The cultivation method adopted in this study was hydroponics, which implied a cultivation method under the condition of sufficient water avoided the restriction of water on the growth and development of tulips. On the other hand, it is necessary to study the differences between various organ indicators of different flowering varieties, such as organ growth rate (Gajanayake et al., 2015), maximum organ growth (Shucun and Lee, 2011), and so on. Therefore, this study provides four tulip growth model parameters at the flowering stage so that the model can accurately predict the growth of different varieties of tulip.

Many tulip studies only showed the management and growth indicators in a qualitative way (Burchi et al., 2010). There was a close relationship between environmental factors and crops that affects photosynthesis and respiration, which affected the growth and development of the crops (Li et al., 2011; Sacks and Kucharik, 2011). Therefore, a quantitative model between environmental factors and growth indicators had a better chance of providing an accurate simulation of crop production. Furthermore, temperature was the key environmental factor affecting crop growth (Maurya and Bhalerao, 2017). There were a number of studies based on the theory of accumulated temperature to simulate crop growth (Elnesr et al., 2013), which had many characteristics, including a simple algorithm, high simulation precision and strong universality. However, because of different crop varieties the required total accumulated temperature of the whole growth process was not the same, the growth model needed to be standardized so that it was more general.

Users can not only use meteorological instruments to directly collect the temperature in the greenhouse, but also predict the temperature in the greenhouse in combination with environmental models (Baxevanou et al., 2010). Through the collected temperature data, the accumulated $Stan_{GDD}$ is calculated. Combined with the growth model algorithm formula constructed in this study, morphology of the growth indicators of each organ of the tulip is calculated. When the optimal selling period of tulips is reached, picking is started. Through this process, the light and temperature resources in the greenhouse can be rationally utilized, and helping users to obtain the greatest economic benefits in production.

While this model provides convenient and accurate production guidance, there are also some parts that need to be improved and perfected. Firstly, the growth model of tulip organs under different water and fertilizer conditions (Souri and Bakhtiarizade, 2019) can be constructed to improve the function of the model. Secondly, the influence of other environmental factors (such as radiation and light length) on the accumulation and distribution of tulip dry matter can be considered. A large amount of experimental data can be collected to verify the model parameters in order to this model would be more versatile. Finally, we can use more advanced data processing methods (such as deep learning), and compare the accuracy of this model with other different model methods to select the best (He et al., 2017).

Conclusions

The results of this study showed that flowering period is not affected by the variety, but the withering period is affect-

ed. In the whole growth and development process of tulips, there was a significant relationship between the growth of fresh cut tulips with different organs and $Stan_{GDD}$, including the Logistic curve, power, linear, quadratic, logarithmic and linear functions. NRMSE of the length index class, area class, proportion class, weight class and SLA simulation model respectively were within the range of 3.40%~29.22%, 17.34%~26.44%, 19.92%~23.85%, 8.26%~24.66% and 9.71%, and RMSE respectively were within the range of 0.25~8.19 cm, 3.36~47.80 cm^2, 0.29~1.86, 0.26~9.58 g $plant^{-1}$ and 1.27 m^2 kg^{-1}. In conclusion, the growth of different organ simulation models had high simulation accuracy.

Acknowledgments

This study was supported by International Training and Improvement Project for Graduate Students of China Agricultural University, Financial Support Project in Beijing, China (PXM2016 151102 000009), Key Laboratory Project of Agricultural Meteorological Security and Applied Technology, China Meteorological Administration (AMF201402), Research Group of the University of Almeria (Spain) (AGR-172), and Soft Science Research Program Project of Zhejiang Province (2022C35063). Thanks to Mr. Haipeng Liu from Landscape Design Department of Beijing International Flower Harbor in China for his support and help with conducting the experiment.

References

Abasi, H., Babalar, M., Lessani, H., and Roohangiz, N. (2015). Effects of nitrogen form of nutrient solution on uptake and concentration macro element and morphological trait in hydroponic tulip. J. Plant Nutr. *39*(12), 1745–1751. https://doi.org/10.1080/01904167.2016.1201110.

Abasi, H., Babalar, M., Lessani, H., and Naderi, R. (2016). Effects of nitrogen form of nutrient solution on uptake and concentration macro element and morphological trait in hydroponic tulip. J. Plant Nutr. *41*(18), 1745–1751. https://doi.org/10.1080/01904167.2016.1201110.

Aghaye Noroozlo, Y., Souri, M.K., and Delshad, M. (2019). Stimulation effects of foliar applied glycine and glutamine amino acids on lettuce growth. Open Agric. *4*(1), 164–172. https://doi.org/10.1515/opag-2019-0016.

Baxevanou, C., Fidaros, D., Bartzanas, T., and Kittas, C. (2010). Numerical simulation of solar radiation, air flow and temperature distribution in a naturally ventilated tunnel greenhouse. Agric. Engin. Intl. CIGR J. *12*(3), 48–67.

Brodribb, T.J., and McAdam, S.A.M. (2017). Evolution of the stomatal regulation of plant water content. Plant Physiol. *174*(2), 639–649. https://doi.org/10.1104/pp.17.00078.

Burchi, G., Prisa, D., Ballarin, A., and Menesatti, P. (2010). Improvement of flower color by means of leaf treatments in lily. Sci. Hortic. *125*(3), 456–460. https://doi.org/10.1016/j.scienta.2010.04.028.

Cerveny, C.B., and Miller, W.B. (2010). Residual effects of ethylene on tulip growth and flowering. HortScience *45*(8), 1164–1166. https://doi.org/10.21273/HORTSCI.45.8.1164.

Cheng, C., Li, Z.F., Dong, C.Y., Gong, Z.H., and Feng, L.P. (2020). Simulation and validation of extinction coefficient at different positions of cucumber and celery in solar greenhouse. Transactions Chinese Soc. Agric. Engin. *36*(21), 243–252.

Douglas, M.H., Smallfield, B.M., Wallace, A.R., and Gimpsey, J.A.M. (2014). Saffron (*Crocus sativus* L.): The effect of mother corm size on progeny multiplication, flower and stigma production. Sci. Hortic. *166*(13), 50–58. https://doi.org/10.1016/j.scienta.2013.12.007.

Elnesr, M.N., Alazba, A.A., and Alsadon, A.A. (2013). An arithmetic method to determine the most suitable planting dates for vegetables. Comp. Electron. Agric. *90*(2), 131–143. https://doi.org/10.1016/j.compag.2012.09.010.

Gajanayake, B., Raja, R.K., and Shankle, M.W. (2015). Quantifying growth and developmental responses of sweetpotato to mid- and late-season temperature. Agron. J. *107*(5), 1854–1862. https://doi.org/10.2134/agronj14.0545.

Garnier, E., Shipley, B., Roumet, C., and Laurent, G. (2010). A standardized protocol for the determination of specific leaf area and leaf dry matter content. Funct. Ecol. *15*(5), 688–695. https://doi.org/10.1046/j.0269-8463.2001.00563.x.

Geng, X.M., Li-Nagasuga, K., Okubo, H., and Saniewski, M. (2005). Effect of TIBA on growth and flowering of non pre-cooled tulip bulbs. Acta Hortic. *673*, 207–214. https://doi.org/10.17660/ActaHortic.2005.673.24.

Greenwood, S., Ruiz-Benito, P., Martínez-Vilalta, J., Lloret, F., Kitzberger, T., Allen, C.D., Fensham, R., Laughlin, D.C., Kattge, J., Bönisch, G., Kraft, N.J., and Jump, A.S. (2017). Tree mortality across biomes is promoted by drought intensity, lower wood density and higher specific leaf area. Ecology Letters *20*(4), 539–553. https://doi.org/10.1111/ele.12748.

Hatamian, M., Rezaei Nejad, A., Kafi, M., Souri, M.K., and Shahbazi, K. (2018). Interaction of lead and nitrate on growth characteristics of ornamental judas tree (*Cercis siliquastrum* L.). Open Agric. *3*, 670–677. https://doi.org/10.1515/opag-2018-0070.

He, D., Wang, E., Wang, J., Lilley, J., Luo, Z., Pan, X., Pan, Z., and Yang, N. (2017). Uncertainty in canola phenology modelling induced by cultivar parameterization and its impact on simulated yield. Agric. Forest Meteorol. *232*, 163–175. https://doi.org/10.1016/j.agrformet.2016.08.013.

Jeung, K.S., and Roh, M.S. (2014). New technique for cut flower production from bulbils of the Asiatic hybrid lily (*Lilium×elegans* Thunb.). Sci. Hortic. *165*(22), 374–383. https://doi.org/10.1016/j.scienta.2013.11.012.

Khan, F.U., Jhon, A.Q., Khan, F.A., and Mir, M.M. (2006). Effect of N, P, K and Zn on growth, flowering and bulb production in tulip under polyhouse conditions in Kashmir. J. Hortic. Sci. *1*(2), 129–134.

Kim, S.H., Niedziela Jr., C.E., Nelson, P.V., Hertogh, A.A.D., and Swallow, W.H., and Mingis, N.C. (2007). Growth and development of *Lilium longiflorum* 'Nellie White' during bulb production under controlled environments. Sci. Hortic. *112*(1), 89–94. https://doi.org/10.1016/j.scienta.2006.11.015.

Korhonen, L., Hadi, Packalen, P., and Rautiainen, M. (2017). Comparison of Sentinel-2 and Landsat-8 in the estimation of boreal forest canopy cover and leaf area index. Rem. Sensing Environm. *195*, 259–274. https://doi.org/10.1016/j.rse.2017.03.021.

Li, G., Chen, Y.R., Dai, J.F., Luo, W.H., Zhao, T.L., and Zhu, P.B. (2011). A model for predicting flowering date and external quality of cut tulip in solar greenhouse. Acta Ecol. Sin. *31*(14), 4062–4071.

Li, X.Y., Zuo, Q.S., Chang, H.B., Bai, G.P., Kuai, J., and Zhou, G.S. (2018). Higher density planting benefits mechanical harvesting of rapeseed in the Yangtze River Basin of China. Field Crops Res. *218*(1), 97–105. https://doi.org/10.1016/j.fcr.2018.01.013.

Liu, S.B. (2015). High effective cultivation technique of tulip. Hortic. & Seed *1*, 55–57.

Maurya, J.P., and Bhalerao, R.P. (2017). Photoperiod and temperature-mediated control of growth cessation and dormancy in trees: A molecular perspective. Ann. Botany *120*(3), 3–10. https://doi.org/10.1093/aob/mcx061.

Nelson, P.V., Kowalczyk, W., Niedziela Jr., C.E., Mingis, N.C., and Swallow, W.H. (2003). Effects of relative humidity, calcium supply,

and forcing season on tulip calcium status during hydroponic forcing. Sci. Hortic. *98*(4), 409–422. https://doi.org/10.1016/S0304-4238(03)00034-7.

Polder, G., Van der Heijden, G.W.A.M., Van Doorn, J., and Baltissen, T.A.H.M.C. (2014). Automatic detection of tulip breaking virus (TBV) in tulip fields using machine vision. Biosyst. Engin. *117*, 35–42. https://doi.org/10.1016/j.biosystemseng.2013.05.010.

Ramírez-Martínez, M., Trejo-Téllez, L.I., Gómez-Merino, F.C., Sánchez-García, P., Rodriguez-Mendoza, M.N., and Sandoval-Villa, M. (2009). Potassium/calcium ratios of the nutrient solution on tulip nutrient status. Acta Hortic. *843*, 119–122. https://doi.org/10.17660/ActaHortic.2009.843.13.

Sacks, W.J., and Kucharik, C.J. (2011). Crop management and phenology trends in the U.S. Corn Belt: Impacts on yields, evapotranspiration and energy balance. Agric. Forest Meteorol. *51*(7), 882–894. https://doi.org/10.1016/j.agrformet.2011.02.010.

Shucun, S., and Lee, E.F. (2011). Flowering phenology and height growth pattern are associated with maximum plant height, relative growth rate and stem tissue mass density in herbaceous grassland species. J. Ecology *99*(4), 991–1000. https://doi.org/10.1111/j.1365-2745.2011.01830.x.

Souri, M.K., and Naiji, M. (2018). Nutritional value and mineral concentrations of sweet basil under organic compared to chemical fertilization. Acta Sci. Pol. Hort. Cultus *17*(2), 167–175. https://doi.org/10.24326/asphc.2018.2.14.

Souri, M.K., and Bakhtiarizade, M. (2019). Biostimulation effects of rosemary essential oil on growth and nutrient uptake of tomato seedlings. Sci. Hortic. *243*, 472–476. https://doi.org/10.1016/j.scienta.2018.08.056.

Xu, R.Y., Niimi, Y., and Han, D.S. (2006). Changes in endogenous abscisic acid and soluble sugars levels during dormancy-release in bulbs of *Lilium rubellum*. Sci. Hortic. *111*(1), 68–72. https://doi.org/10.1016/j.scienta.2006.08.004.

Zhang, D.S., Li, X.F., and Wang, P. (2009). The character and analysis of the growth of tulips in Jinan region. Chin. Landscape Architect. *25*(5), 80–83.

Received: Mar. 9, 2021
Accepted: Jul. 30, 2021

Addresses of authors:
Chen Cheng[1,2], Liping Feng[2,*] J.F. Bienvenido Barcena[3], Weidong Yu[4], Gen Li[5], Zhenfa Li[5] and Caihua Ye[6,**]
[1] Institute of Ecology, Lishui University, Lishui, Zhejiang, 323000, China
[2] College of Resources and Environment Sciences, China Agricultural University, Beijing, 100193, China
[3] Computer Science Department, University of Almeria, Almeria, 04120, Spain
[4] CMA/Henan Key Laboratory of Agro-meteorological Support and Applied Technique, Zhengzhou, 450003, China
[5] Tianjin Climate Center, Tianjin, 300074, China
[6] Beijing Municipal Climate Center, Beijing, 100089, China
Corresponding authors; E-mail:
* : fenglp@cau.edu.cn
**: ych681012@126.com